Understanding the Complex Phase Diagram of Uranium: The Role of Electron-Phonon Coupling

S. Raymond,[1] J. Bouchet,[2] G. H. Lander,[3] M. Le Tacon,[4,5] G. Garbarino,[4] M. Hoesch,[4] J.-P. Rueff,[6,7] M. Krisch,[4] J. C. Lashley,[8] R. K. Schulze,[8] and R. C. Albers[8]

[1]*SPSMS, UMR-E 9001, CEA-INAC/UJF-Grenoble 1, 38054 Grenoble, France*
[2]*CEA, DAM, DIF, F-91297 Arpajon, France*
[3]*European Commission, Joint Research Centre, Institute for Transuranium Elements, Postfach 2340, D-76125 Karlsruhe, Germany*
[4]*European Synchrotron Radiation Facility, Boite postale 220X, F-38043 Grenoble, France*
[5]*Max-Planck-Institut für Festkörperforschung, Heisenbergstraße 1, D-70569 Stuttgart, Germany*
[6]*Synchrotron SOLEIL, L'Orme des Merisiers, Saint Aubin, BP 48, 91192 Gif-sur-Yvette Cedex, France*
[7]*Laboratoire de Chimie Physique—Matière et Rayonnement, CNRS-UMR 7614, UPMC, 75005 Paris, France*
[8]*Los Alamos National Laboratory, New Mexico 87545, USA*

(Received 4 March 2011; published 21 September 2011)

We report an experimental determination of the dispersion of the soft phonon mode along [100] in uranium as a function of pressure. The energies of these phonons increase rapidly, with conventional behavior found by 20 GPa, as predicted by recent theory. New calculations demonstrate the strong pressure (and momentum) dependence of the electron-phonon coupling, whereas the Fermi-surface nesting is surprisingly independent of pressure. This allows a full understanding of the complex phase diagram of uranium and the interplay between the charge-density wave and superconductivity.

DOI: 10.1103/PhysRevLett.107.136401 PACS numbers: 71.45.Lr, 63.20.kd, 74.25.Kc

Competition between different ground states is a central issue in condensed-matter physics. Much-discussed examples are those between superconductivity and magnetism in cuprates, iron pnictides, and heavy fermions. Equally important is that between the charge density wave (CDW) and superconductivity, as shown by recent progress reported for the transition-metal chalcogenides [1,2] and elements under pressure [3]. The present paper sheds new light on the mechanisms that govern such an interplay between CDW and superconductivity in uranium. At ambient pressure, uranium is the only element to exhibit a phase transition to a CDW state below $T_0 = 43$ K [4,5]. This transition has been ascribed to nesting of certain features of the Fermi surface [6]. The ambient pressure superconductivity of uranium, reported in the early studies [4] below 1 K, is still controversial [7], but it is agreed that the superconducting temperature T_c exhibits a maximum of about 2 K at around 1.5 GPa, when the CDW disappears [4].

The room temperature crystal structure of uranium is of much interest, since it is unique for an element at ambient pressure. Uranium exists in an unusual orthorhombic structure (α-U phase, space group *Cmcm*) [4] and adopts this structure to at least 100 GPa [8]. Similar orthorhombic structures are found in Ce [9], Pa, Am, and Cm [10] at higher pressures and are understood as a consequence of the f electrons in these materials being squeezed into itinerant states at high pressure. The key aspect, which stabilizes the low-symmetry orthorhombic α-U structure [11], is the narrow band (2–3 eV wide) containing about three $5f$ electrons at the Fermi level. At low temperature, the CDW state to a first approximation may be considered as a doubling of the a axis of the unit cell, and this structure is called α_1-U.

Recent progress in band structure calculations allows the accurate determination of the phonon spectrum of actinide-based materials [12,13]. Treating the $5f$ electrons as itinerant, the unusual phonon spectrum of α-U was reproduced only in 2008 by *ab initio* calculations [14], almost 30 years after its experimental determination [15]. Importantly, these calculations incorporate all $5f$ electrons as itinerant in the correct orthorhombic α-U structure. If the number of $5f$ states is varied or the incorrect crystal structure used, the soft phonon in the Σ_4 branch is *not* reproduced [14]. A prediction of this calculation is that under pressure the energy of the soft phonon with Σ_4 symmetry [15] in the [100] direction *increases*, until the anomaly disappears near 20 GPa. In the present paper, we report inelastic x-ray scattering (IXS) data that confirm the major changes predicted in the phonon spectra on applying pressure, thus benchmarking the theory. The quantitative agreement between experiment and theory encourages us to perform new calculations aiming to understand the complex phase diagram of uranium at low temperature. As a function of pressure, the increase in energy of the soft mode is tied directly to changes in the electron-phonon (e-ph) coupling, whereas, surprisingly, the Fermi-surface nesting remains unaltered.

The IXS experiments were performed on a single crystal sample at the beam line ID28 at the European Synchrotron Radiation Facility in Grenoble, France, and the theoretical calculations were performed using density functional theory. Details of the experimental and theoretical methods are given in the Supplemental Materials, Parts I and II [16].

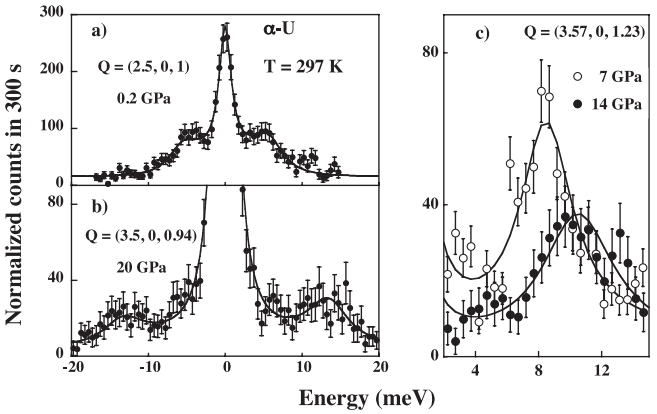

FIG. 1. IXS data at ambient temperature taken for $\mathbf{q} \approx (0.5, 0, 0)$. Data show both the energy-loss (Stokes) and energy-gain (anti-Stokes) response, as well as the central elastic line at the lowest (a) and highest (b) pressure measured. (c) Zoom on the Stokes peak for intermediate pressures.

Figure 1 shows IXS spectra for different pressures around the key positions in reciprocal space. In this Letter, we indicate the momentum transfer $\mathbf{Q} = \tau + (h, k, l)$, where τ is a reciprocal lattice vector. It is known from earlier studies [4,15], as well as theory [14], that the Σ_4 phonon energies are not strongly dependent on the coordinate l along the [001] axis; thus, we are interested primarily in the h parameter along [100]. The data shown in Fig. 1 establish the hardening (increase of energy) of the Σ_4 mode as pressure is increased. Figure 2(a) shows the dispersion along the important [100] direction for three pressures for data taken at $\mathbf{q} = (h, 0, l)$ with $0 \leq l \leq 0.2$. The minimum is known to occur for $h \approx 0.5$ [4,15]. Figure 2(b) shows the soft-mode energy as a function of pressure. Our data confirm the disappearance of the soft mode under pressure as predicted by Bouchet [14] (Supplemental Materials, Part III [16]). When the pressure was released from 20 to 6 GPa, the soft mode was found reversible with pressure [see Fig. 2(b)].

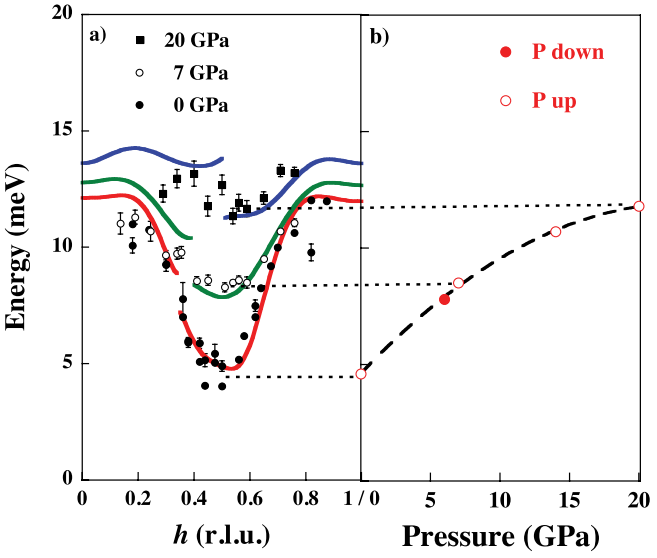

FIG. 2 (color online). Phonon energy: (a) Experimental (data points with error bars) and theoretical (solid lines) dispersion of the Σ_4 optic component along [100]. (b) Soft-mode energy as a function of pressure (lines are guides for the eyes).

So far, theory and experiments have referred to the orthorhombic α-U structure. The excellent agreement between theory and experiment prompted a further examination of the pressure and temperature dependence of parameters that define this structure and that of the CDW (α_1-U). We calculated the complete band structure for both α-U and α_1-U, their phonon dispersion curves, and, importantly, the $\mathbf{q}$-dependent e-ph coupling $\lambda_{\mathbf{q},\nu}$ with

$$\lambda_{\mathbf{q},\nu} = \frac{2\gamma_{\mathbf{q},\nu}}{\pi N(0)(\hbar\omega_{\mathbf{q},\nu})^2}, \tag{1}$$

where $N(0)$ is the density of states at the Fermi level, $\hbar\omega_{\mathbf{q},\nu}$ is the phonon energy at wave vector $\mathbf{q}$ and phonon mode index ν, and $\gamma_{\mathbf{q},\nu}$ is the mode-resolved linewidth (in energy units) resulting from the e-ph coupling

$$\gamma_{\mathbf{q},\nu} = 2\pi\hbar\omega_{\mathbf{q},\nu}\sum_{\mathbf{k}}|M^{\nu}_{\mathbf{k}+\mathbf{q},\mathbf{k}}|^2\delta(\epsilon_{\mathbf{k}})\delta(\epsilon_{\mathbf{k}+\mathbf{q}}), \tag{2}$$

where $M^{\nu}_{\mathbf{k}+\mathbf{q},\mathbf{k}}$ is the e-ph matrix element, $\epsilon_{\mathbf{k}}$ are the electron eigenvalues, and the sum runs over the Brillouin zone [17,18].

By examining the phonons and the e-ph coupling, we extract new details about the phase diagram. The key parameters for the Σ_4 mode in the α-U structure as a function of momentum transfer along the [100] direction and, for different pressures, are shown in Fig. 3. Figure 3(a) shows the phonon dispersion, Fig. 3(b) shows the e-ph coupling specific to this mode $\lambda_{\mathbf{q},\nu}$, and Fig. 3(c) shows the phonon linewidth due to e-ph interaction. The strong dependence along [100] implies that the major difference of the α_1-U (CDW) from the stable α-U structure will be along this direction. The total energy calculations (at $T = 0$ K) show that the ground state at ambient pressure is the α_1-U (CDW), and the crossover to the normal α-U structure is calculated to be at just over 1 GPa. When fully relaxing the α_1-U structure, small components are also found theoretically along [010] and [001], in agreement with experiment [4]. The parameter $\gamma_{\mathbf{q},\nu}$ is closely connected to the nesting features of the Fermi surface. Clearly, these reach a maximum near the middle of the Brillouin zone along [100]; however, in contrast to $\lambda_{\mathbf{q},\nu}$, they do not depend strongly on pressure. We have investigated the Fermi-surface nesting further, as shown in Fig. 4(a) at ambient pressure and in Fig. 4(b) at 20 GPa. First, the Fermi surface at ambient pressure closely resembles Fig. 4 of Ref. [6] with a nesting vector of magnitude $k_x \approx 0.5(2\pi/a)$ (Supplemental Materials, Part IV [16]). Second, comparing Figs. 4(a) and 4(b), there is essentially no change as a function of pressure. This central result, that we confirmed with two independent calculations, is unexpected. Thus, the

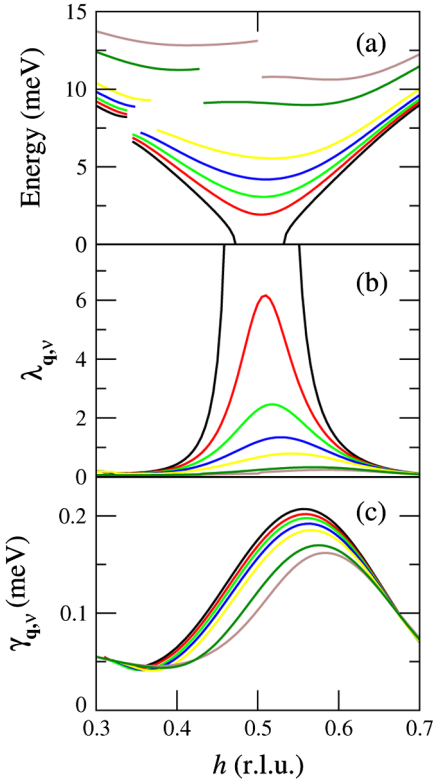

FIG. 3 (color online). Results of calculations at $T = 0$ K using the experimental volume (see the Supplemental Materials, Part II [16]): (a) Energy of the Σ_4 phonon mode along [100]. (b) The e-ph coupling, $\lambda_{\mathbf{q},\nu}$. (c) The phonon linewidth due to e-ph interaction, $\gamma_{\mathbf{q},\nu}$. The different pressures are 0, 0.8, 2.5, 5.1, 10.3, 16, and 25 GPa from bottom to top in (a) and from top to bottom in (b),(c).

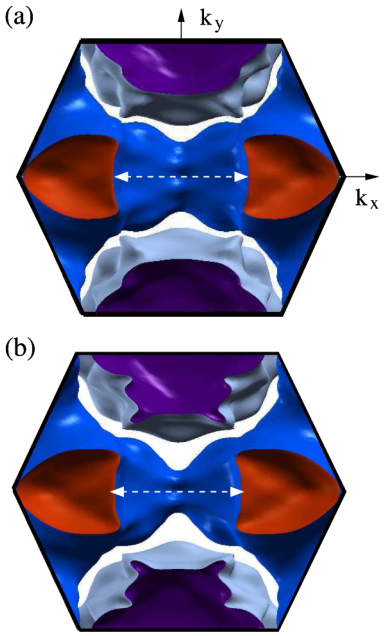

FIG. 4 (color online). The Fermi-surface topology for the α-U structure calculated at (a) ambient pressure and (b) at 20 GPa. In each case, the diagram shows the [100] and [010] axes at a fixed position $z = 1/2$ along [001]. The different colors correspond to the different sheets of the Fermi surface. The arrow indicating the nesting vector {$\approx 1/2(2\pi/a)$ along [100]} has been drawn the same length in both (a) and (b).

statement that the CDW in uranium is a consequence of the nesting of the Fermi surface is incorrect, as the CDW is rapidly destroyed by pressure, disappearing by ≈ 1.5 GPa [4], whereas the nesting does not change.

Indeed, Fermi-surface nesting is present, but, although necessary, this is not the unique ingredient for the formation of the α_1-U (CDW) state; otherwise, this phase would not be so sensitive to pressure. The crucial ingredient is the e-ph coupling which allows transferring the energy gain from nesting in the CDW state to the lattice. At high pressure, the CDW will not develop, as the e-ph coupling is too weak to transmit the electronic information to the lattice. These conclusions are consistent with the arguments of Johannes and Mazin [19], who stress that in most cases such phase transitions cannot be ascribed to Fermi-surface nesting alone. Our calculations for the phonons in the distorted α_1-U structure (which contains 8 atoms in the unit cell, rather than the 4 in the α-U structure) show that the choice for the displacements made previously [6] does not result in finite energies for the Σ_4 mode phonons. To correct this, we need to preserve the C-face centering in the distorted α_1-U phase. This gives a lower total energy when compared to the α_1-U structure adopted in [6].

Finally, we address the fascinating interplay between the CDW and superconductivity, as shown in Fig. 5. The open triangles and squares in Fig. 5, traced by the solid line, mark the experimental pressure dependence of T_c [4]. In order to calculate T_c, given our knowledge of the e-ph coupling, we use the formula of McMillan [20]:

$$T_c = \frac{\theta}{1.45} \exp\left(-\frac{1.04(1+\lambda)}{\lambda - \mu^*(1+0.62\lambda)}\right), \qquad (3)$$

where θ is the Debye temperature, λ is the mass renormalization factor (average e-ph coupling; see [17,18]), and μ^* is the e-ph repulsion term. The calculation of λ is complex near the transition from the α to α_1 phases, due to its large values, and the experimental uncertainties about the nature of the atomic displacements, so it is convenient to anchor the calculations of T_c to the experimental value of $T_c = 1.5$ K at 3 GPa. This gives a value for μ^* of 0.28. μ^* is typically 0.1 for simple metals and 0.13 for transition metals, but narrow bands, as in $5f$ electron systems, can give rise to large μ^* [21]. We then deduce (keeping μ^* fixed and using $\lambda_{\mathbf{q},\nu}$ from the calculation) T_c in the α-U state, and these values are shown as solid circles in Fig. 5. Since λ strongly reduces with increasing pressure, it is not surprising that T_c also decreases, exactly as found experimentally. For $\lambda_{\mathbf{q},\nu}$ in the CDW (α_1-U) state, on the other hand, the opposite behavior occurs: it increases as a function of pressure. Indeed, for ambient pressure, the Σ_4 phonon

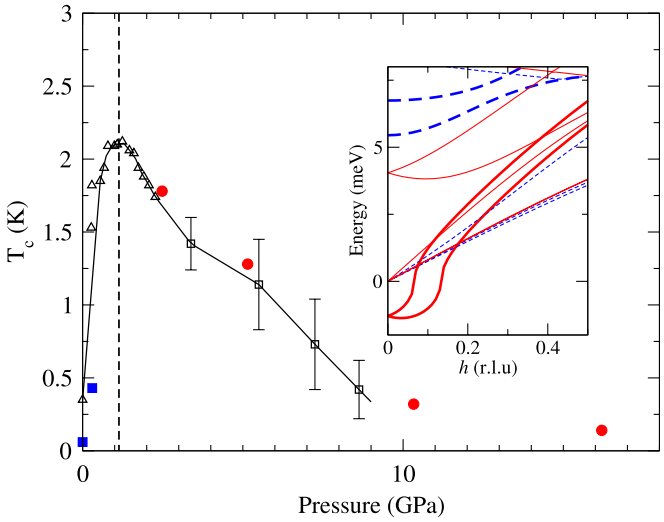

FIG. 5 (color online). T-P phase diagram of uranium in the superconducting region. The vertical dashed line (at 1.2 GPa) indicates the calculated transition between the CDW phase and the normal α-U structure in good agreement with experiment. The experimental T_c values, taken from Fig. 3.3 of Ref. [4], are indicated by open triangles and squares, and the solid line is a guide for the eyes. The calculated values are shown as solid squares (α_1) and solid circles (α-U) and were scaled at 3 GPa (see text). The inset shows the phonon dispersion curves in the CDW state (α_1 structure) for zero pressure (dashed lines) and 5 GPa (solid lines). The thicker lines are the branches corresponding to the Σ_4 mode in the α-U phase.

modes, which are now at the zone center (Γ) of the new, much smaller, Brillouin zone, have a finite energy, and, as the pressure is increased, the phonon modes decrease in energy. The calculations in the inset of Fig. 5 show the low energy phonons in the CDW state at zero and 5 GPa. By the latter pressure, the predicted acoustic phonon energies are negative, showing that the structure is unstable. Thus, initially $\lambda_{\mathbf{q},\nu}$ increases with increasing pressure in the CDW state, leading to an increase in T_c, as shown by the solid squares in Fig. 5, and finally gives the maximum in T_c at the phase transition. Qualitatively, this reproduces satisfactorily the experimentally observed behavior. The corresponding parameters λ and θ are given in Table I for both α_1-U and α-U. The obtained λ values are qualitatively consistent with the ones found in the literature for similar μ^* at ambient pressure [21] and at around 1 GPa [4].

Our calculations show that the momentum and pressure dependence of the e-ph coupling plays the central role in determining the complex phase diagram of uranium. The predictions of the theory about the anomalous phonons are verified by experiment (Fig. 3). However, since the Fermi-surface nesting is independent of pressure (Fig. 4), this alone cannot explain the formation of the CDW [19]. In addition, the theory succeeds in explaining the appearance of the CDW at base temperature and ambient pressure (Fig. 3). It predicts (as observed experimentally) that the CDW will be unstable at 1.2 GPa (Fig. 5). Using the McMillan formula, the pressure dependence of T_c is explained (Fig. 5), as well as its absolute value, assuming a reasonable value for the electron-repulsion term and phonon-mediated Cooper pairing.

TABLE I. Pressure dependence of the mass renormalization factor (λ), Debye temperature (θ), and corresponding T_c for $\mu^* = 0.28$. The calculation is made for α_1-U (solid squares in Fig. 5) and for α-U (solid circles in Fig. 5).

	α_1-U		α-U			
P (GPa)	0	0.3	2.5	5.1	10.3	16.2
λ	0.60	0.72	0.90	0.77	0.70	0.64
θ (K)	182	182	183	184	185	190
T_c (K)	0.06	0.43	1.78	1.28	0.32	0.14

The present joint experimental and theoretical investigation has allowed important progress in understanding the complex phase diagram of uranium. Moreover, our study lays the foundation for further extension of theory into strongly correlated systems.

[1] E. Morosan *et al.*, Nature Phys. **2**, 544 (2006) and references therein.
[2] M. Calandra and F. Mauri, Phys. Rev. Lett. **106**, 196406 (2011).
[3] O. Degtyareva *et al.*, Phys. Rev. Lett. **99**, 155505 (2007) and references therein.
[4] G. H. Lander *et al.*, Adv. Phys. **43**, 1 (1994) and references therein.
[5] Chromium exhibits a spin-density wave with an induced CDW. Other elements exhibit a CDW at elevated pressure; see M. I. McMahon and R. J. Nelmes, Chem. Soc. Rev. **35**, 943 (2006).
[6] L. Fast *et al.*, Phys. Rev. Lett. **81**, 2978 (1998).
[7] See D. Graf *et al.*, Phys. Rev. B **80**, 241101 (2009).
[8] T. Le Bihan *et al.*, Phys. Rev. B **67**, 134102 (2003).
[9] F. H. Ellinger and W. H. Zachariasen, Phys. Rev. Lett. **32**, 773 (1974).
[10] S. Heathman *et al.*, Science **309**, 110 (2005).
[11] P. Söderlind *et al.*, Nature (London) **374**, 524 (1995).
[12] X. Dai *et al.*, Science **300**, 953 (2003).
[13] S. Raymond *et al.*, Phys. Rev. Lett. **96**, 237003 (2006).
[14] J. Bouchet, Phys. Rev. B **77**, 024113 (2008).
[15] W. P. Crummett *et al.*, Phys. Rev. B **19**, 6028 (1979).
[16] See Supplemental Material at http://link.aps.org/supplemental/10.1103/PhysRevLett.107.136401 for experimental and theoretical methods, as well as for precise details on phonon linewidth and Fermi-surface nesting.
[17] A. Y. Liu and A. A. Quong, Phys. Rev. B **53**, R7575 (1996).
[18] S. Y. Savrasov and D. Y. Savrasov, Phys. Rev. B **54**, 16487 (1996).
[19] M. D. Johannes and I. I. Mazin, Phys. Rev. B **77**, 165135 (2008).
[20] W. L. McMillan, Phys. Rev. **167**, 331 (1968).
[21] H. L. Skriver *et al.*, Phys. Rev. B **37**, 1706 (1988) and references therein.